DNS OF STRIPE PATTERN IN POISEUILLE FLOW
AT VERY LOW REYNOLDS NUMBER

Koji Fukudome, Yoshifumi Ogami
Department of Mechanical Engineering
Ritsumeikan University
1-1-1 Noji-higashi, Kusatsu, Shiga, 525-8577, Japan
fukudome@cfd.ritsumei.ac.jp, y_ogami@cfd.ritsumei.ac.jp

ABSTRACT

Direct numerical simulations (DNSs) of a spectral method were performed to study the turbulent structure in a transitional regime in Poiseuille flow. A computational domain tilted towards the streamwise direction was adopted at a high aspect ratio. Though the simulations, turbulent stripes consisting of turbulent and quasilaminar regions were obtained for various values of the angle θ of the stripe with respect to the streamwise direction. The flow rate in the streamwise direction attained a local minimum at $\theta = 20°$, although the flow rate in the spanwise direction attained a maximum at this angle. Moreover, the stripe at $\theta = 20°$ became temporally steady for least $t^+ < 2800$ without lateral spreading. Both the widths and intervals of the turbulent regions are well normalized by the streamwise distance at $\theta = 10$–$35°$. Furthermore, the width of the turbulent region measured perpendicular to the stripe at $\theta = 20°$ is consistent with the highly dissipating region in the homogeneous flow at a very high Reynolds number.

INTRODUCTION

In the transitional regime, the flow is known to be spatially intermittent, consisting of turbulent and quasilaminar regions. A turbulent stripe is one of the intermittent flow structures in which the turbulent and quasilaminar regions are alternately arrayed in the streamwise and spanwise directions and form a stripe pattern. The turbulent stripe was firstly discovered in the experimental study of Taylor–Couette flow by Coles (1965, 1966). Then, stripes were experimentally observed in a Couette flow by Prigent et al. (2002) and studied numerically by Barkley (2005); similarly, stripes were numerically studied in a Poiseuille flow by Tsukahara et al. (2005, 2007) and experimentally observed (Tsukahara et al., 2010a, Seki et al., 2010, 2012). Additionally, a similar stripe was also found in a torsional Couette flow by Cros et al. (2002). Therefore, turbulent stripes are a common flow state in a flow bounded by parallel walls at the transitional Reynolds number. Further, the turbulent structures of the stripes in various shear flows are common; for instance, the turbulent region evolves many vortical structures, and high- and low-speed fluids are distributed upwind and downwind in turbulent regions, respectively.

In Poiseuille flow, Iida and Nagano (1998) carried out DNSs of Poiseuille flows in the transitional regime in a small computational domain and found temporal oscillations in the flow rates and friction coefficients. Although they could not capture the turbulent stripe because of their small computational domain, Tsukahara et al. (2005, 2006, 2007) carried out DNSs a large computational domain, captured the stripe structure, and studied the mean structure of the stripes inclined at 21° with respect to the streamwise direction in a very huge computational domain. Duguet et al. (2010) studied the appearance of turbulent stripes in Couette flows and concluded that a stripe was obtained from both a single point disturbance and a homogeneous disturbance, such that turbulent stripes appear naturally and generally. Philip and Manneville (2011) clarified that the turbulent stripes and the temporal evolution in Couette flows were affected by the computational domain. Manneville (2011, 2012) observed the development and decay of turbulent stripes in Couette flows by changing the Reynolds number by numerical simulation. Fukudome and Iida (2012) also clarified the turbulent stripe in Poiseuille flows and suggested the sustaining mechanism for which the tilting of the mean shear is important. Duguet et al. (2013) also suggested the maintaining mechanism and mathematical models for the stripe. On the other hand, a turbulent stripe was observed at much higher Reynolds numbers with the addition of a stable body force and confirmed by Tsukahara et al. (2010b) and Brethouwer et al. (2013).

According to previous research, the turbulent stripes in various shear flows have a common feature in that the stripes incline towards the spanwise direction from the streamwise direction, and the turbulent regions are sandwiched by high- and low-speed fluid on the upwind and downwind sides. In this study, we performed direct numerical simulations of the Poiseuille flow in the transitional regime to clarify the inclination angle and the space interval of the stripes.

NUMERICAL PROCEDURE

The objective flow field is the Poiseuille flow shown in Figure 1, where x and z are spanwise directions parallel and perpendicular, respectively, to the stripe pattern, and y is the wall-normal direction. This method was used by Barkley and Tuckerman (2005) for a Couette flow, as shown in Figure 2. In this study, we adopt a large aspect ratio in the plane horizontal to the z direction, i.e., the nonhomogeneous direction, to eliminate the effect of the computational domain size, as shown in Figure 3. The
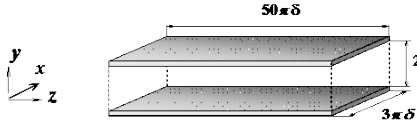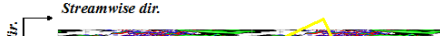
Figure 1. Configuration of the computational domain.

flow is driven by a constant mean pressure gradient in the streamwise direction, where the streamwise direction is tilted in the x direction at $\theta = 0\text{–}85°$ every $5°$. Periodic boundary conditions are imposed in the x and z directions, whereas the no-slip boundary condition is imposed on the walls. Hence, we think that the obtained intervals of the turbulent regions will behave more naturally. The numerical method used in this study is the Chebyshev and Fourier spectral method used by Kim et al. (1987) and Fukudome and Iida (2012). For the time integration, the second-order Adams–Bashforth and Crank–Nicolson schemes are adopted for the nonlinear and viscous terms, respectively. The DNSs in the present work are $Re_\tau = 70$ with a computational domain of $3\pi\delta \times 2\delta \times 50\pi\delta$ with a $96 \times 65 \times 1728$ grid system. Here, the friction Reynolds number Re_τ is defined by the friction velocity u_τ and channel half width δ. As the initial condition, a fully developed Poiseuille flow at $Re_\tau = 100$ is calculated in advance and the Re_τ of the flow is systematically decreased to 70. The superscript + represents normalization using u_τ and the kinetic viscosity ν. The time step is $\Delta t^+ = 0.035$.

RESULTS AND DISCUSSION

Figure 4 shows the distribution of the vortical structure identified by *II* and the streamwise velocity in the channel center. In all cases, the vortical structures were gathered and periodically arrayed in the z direction. For $\theta = 0°$ (Figure 4(a)), high- and low-speed regions at the channel's center and vortical structures array in the streamwise direction. For $\theta = 20°$ (Figure 4(b)), each of the turbulent and quasilaminar regions greatly expand, and high- and low-speed fluids exist upwind and downwind in turbulent regions, respectively. For $\theta = 40°$ and $60°$ (Figure 4(c, d)), the vortical structure clusters in the streamwise direction, and the intensities of the high- and low-speed fluids becomes weaker. Moreover, the boundary between the turbulent and laminar regions becomes obscured. As the high- and low-speed fluids in the upwind and downwind turbulent regions form strongly and widely at $\theta \sim 20°$, the turbulent regions can be sustained. This result is consistent with previous studies (Tsukahara et al. 2005, Duguet et al. 2013, Tuckerman et al., 2014).

Figure 5 shows the flow rates in the streamwise and spanwise directions as a function of θ. The flow rates are defined by the channel width 2δ and the mean velocity in the streamwise and spanwise directions. The streamwise flow rate Re_m attains a minimum and maximum at $\theta = 0°$ and $5°$ degrees, respectively. At $\theta = 20°$, the flow rate attains a local minimum, such that a Reynolds stress was produced vigorously. On the other hand, the spanwise flow rate Re_w peaks at $\theta = 20\text{–}25°$, and this spanwise flows occurs because of the circulating flows along the turbulent regions consisting of high- and low-speed fluids in the upwind and downwind turbulent regions, respectively. Therefore, the strong circulation along the turbulent regions is at $\theta \sim 20°$. As a result, strong circulation and a Reynolds stress are generated at $\theta \sim 20°$ such that the turbulent stripes inclined at $\theta \sim 20°$ with respect to the streamwise direction seem to be very realizable, which is consistent with previous results (Tsukahara et al. 2010). In the simulations, a laminar state was not obtained; thus, the computational domain is much larger than the minimal flow unit (Jiménez and Moin, 1991).

Figure 6 shows the time evolution of the turbulent regions indicated by the dissipation rate averaged at each z plane. Here, the z position moves with the turbulent region. In all cases, regions of high-dissipation-rate exist locally and are consistent with the turbulent regions. For $\theta = 0°$ (Figure 6(a)), high-dissipation-ratio regions appear and
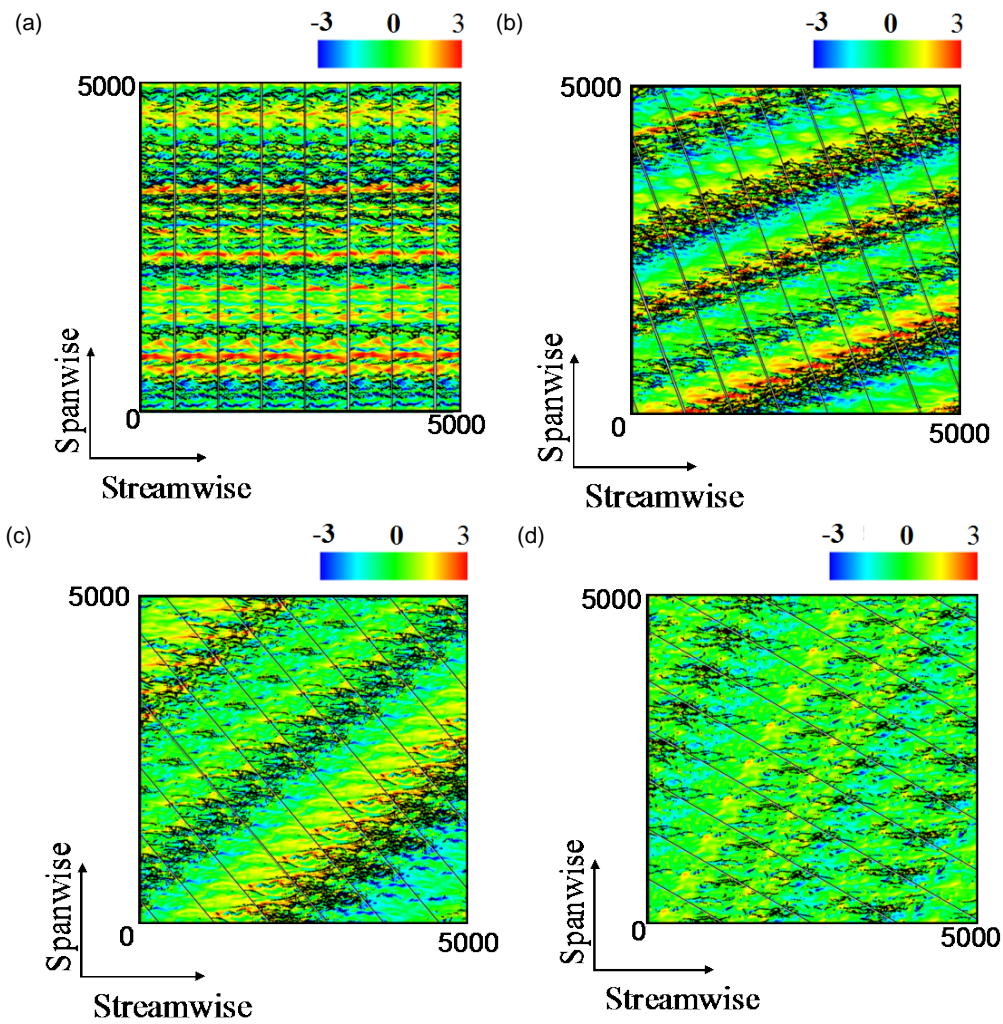
Figure 4. Instantaneous flow structures of high- and low-speed fluids at the channel center and the vortical structure in the entire channel viewed from the top. The black isosurfaces represent the vortical structure identified by the second invariant of the velocity gradient tensor $II^+=0.001$. The red and blue contours represent the streamwise velocity fluctuation $u'^+ = -3$ to 3. Black thin lines show the boundaries of the computational domains. The computational domains that are indicated by thin lines are repeated periodically in the x direction. (a) $\theta = 0$ degree. (b) $\theta = 20$ degree. (c) $\theta = 40$ degree. (d) $\theta = 60$ degree.
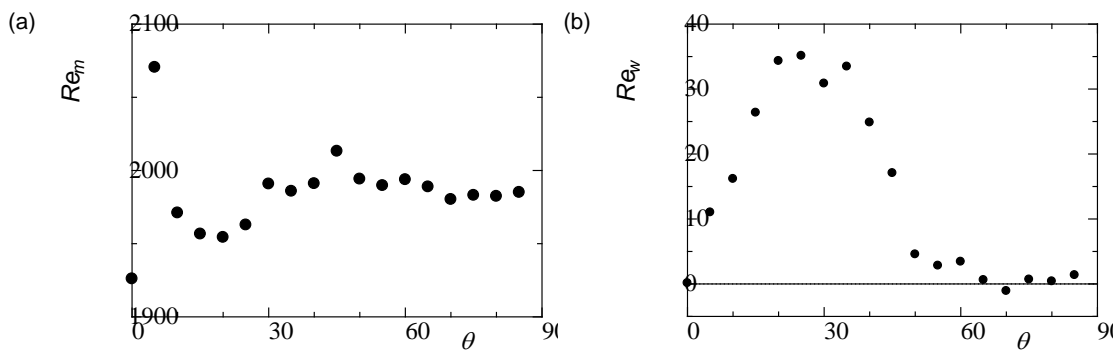

Figure 5. Flow rates in the (a) streamwise Re_m and (b) spanwise Re_w directions, respectively. Re_m and Re_w are defined by the channel width 2δ and the mean velocities along the streamwise and spanwise directions, respectively.
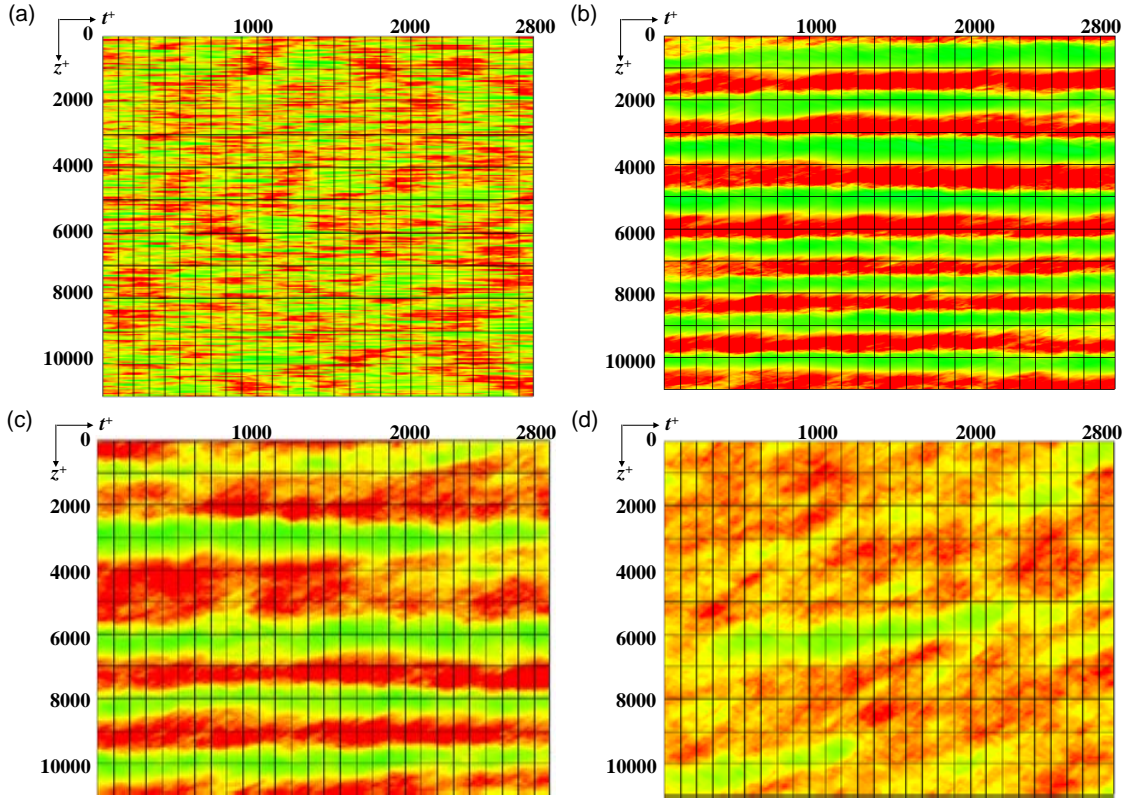
3

Figure 6. Temporal evolution of the turbulent regions identified by the dissipation rate averaged at the z-plane. The blue and red contours represent the local averaged dissipation rate $\varepsilon^+ = 0$ to 2.5 . (a) $\theta = 0°$. (b) $\theta = 20°$. (c) $\theta = 40°$. (d) $\theta = 60°$.
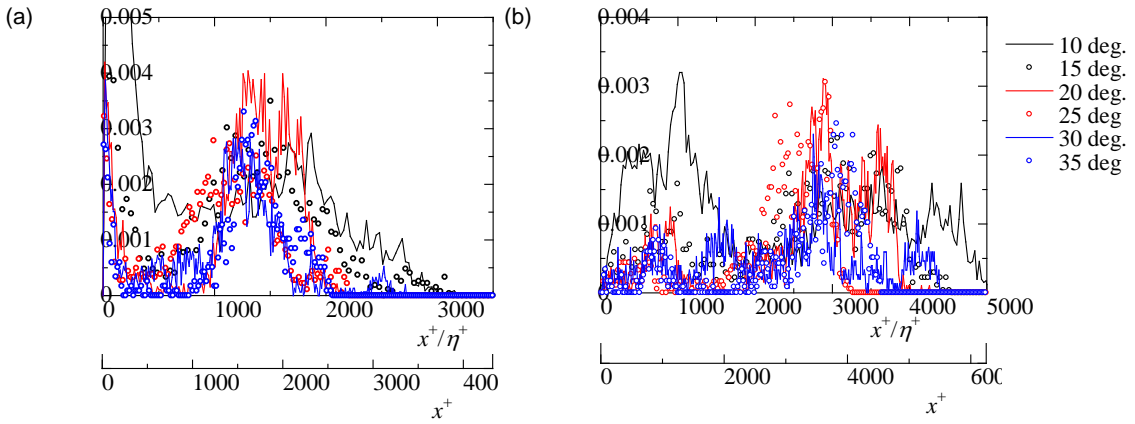

Figure 7. The probability density functions of the lengths and the intervals of the turbulent region in the streamwise direction for $\theta = 10$–$35°$. The turbulent regions are identified by the region where the local averaged dissipation rates shown in Figure 6 take higher than the average values in the entire channel.

disappear locally with time, and the width of the region is narrow in the spanwise direction. In case of $\theta = 20°$ (Figure 6(b)), turbulent regions indicating high dissipation ratios exist periodically in the z direction, and are steady in time for $t^+ > 2800$. Lateral spreading (Shi et al., 2013),

in which the turbulent region is divided into two, is not observed here. For $\theta = 40°$ (Figure 6(c)), the turbulent regions become wider in the z direction than for $\theta = 20°$. The number of the turbulent regions does not change temporally, although the intensity of the dissipation ratio
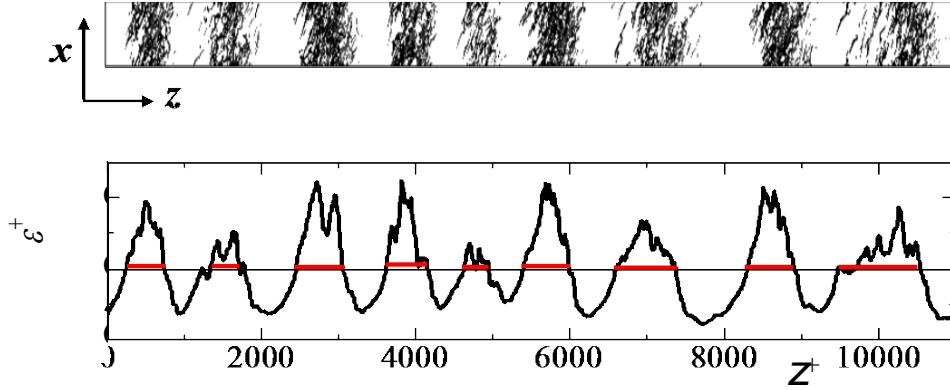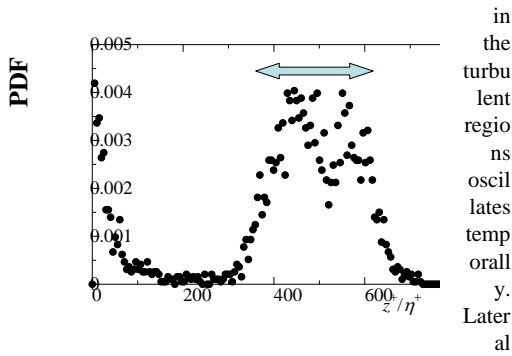
4

Figure 8. Instantaneous distribution of the longitudinal vortices in the computational domain (top) and the dissipation rate (bottom) for $\theta = 20°$. In the top figure, the vortical structure is same as that in Figure 4. In the bottom figure, the dissipation ratio is averaged over x–y plane at each z location. The thin lines represent the mean value in the entire channel which is 0.2. The thick red lines indicate the identified turbulent regions.

spreading is observed. For $\theta = 60°$ (Figure 6(d)), the interface between the turbulent and quasilaminar regions become unclear, and lateral spreading of the turbulent regions is observed frequently. The probability of lateral spreading seems to be affected by the angle of the turbulent regions.

Figure 7 shows the probability density functions (PDFs) of the lengths and intervals of the turbulent region in the streamwise direction for $\theta = 10$–$35°$. These lengths are measured in the streamwise direction. The PDFs of the lengths of the turbulent regions in the streamwise direction peak at $x^+ = 1000$ to 1500 in all cases. In addition, the PDFs of the intervals of the turbulent regions in the streamwise direction peak at $x^+ = 3000$ to 4000 in all cases. As a result, the scales of the turbulent stripe are well normalized by the length in the streamwise direction.

Figure 8 shows the instantaneous distribution of the vortical structure and the dissipation rate averaged at the z plane for $\theta = 20°$. The average value of the dissipation rate ε^+ is 0.2 in the entire channel. As indicated in Figure 6, the turbulent regions consisting of many vortical structures are consistent with the regions indicating a high dissipation rate. The width of the turbulent regions in the z direction, where the dissipation rate is higher than the mean value is almost $z^+ = 600$–800, which is consistent in the turbulent regions oscillates temporally. Lateral

with $z^+/\eta^+ = 400$–600. Figure 9 shows the PDF of the width of the turbulent region averaged from $t^+ = 0$ to 2800. The horizontal axis is normalized by the Kolmogorov length scale η. The peak is located in the $z^+/\eta^+ = 400$–600.

Ishihara et al. (2011) found a high dissipating region in homogeneous turbulence. The region consists of many vortical structures and circulating flow along the region, such that the turbulent structure resembles a turbulent stripe. The width of the region in homogeneous turbulence is comparable to that of a turbulent stripe in the present study. We consider that the turbulent stripe is very similar to the high shear region observed in a homogeneous flow with a very high Reynolds number from the viewpoints of kinematics and the scale normalized by the Kolmogorov scale.

CONCLUSION

Direct numerical simulations were performed to study the structure of a turbulent stripe in a Poiseuille flow. A computational domain tilted towards the streamwise direction was adapted at a laterally high aspect ratio. As a result, we obtained the following.

1. To adopt the tilted computational domain, turbulent stripes consisting of turbulent and quasilaminar regions were obtained for various angles of the stripe in the streamwise direction.
2. The flow rate in the streamwise direction attains a local minimum at $\theta = 20°$, although the flow rate in the spanwise direction attains a maximum at this angle.
3. The stripe at $\theta = 20°$ becomes temporally steady for $t^+ < 2800$ without lateral spreading. Lateral spreading was obtained for $\theta > 40°$.
4. Both the widths and intervals of the turbulent regions are well normalized by the streamwise distance at each angle θ.

5

5. The width of the turbulent region measured perpendicular to the stripe is consistent with the highly dissipating region in a homogeneous flow at a very high Reynolds number.

REFERENCES

Barkley, D., and Tuckerman, L. S., 2005, "Computational study of turbulent laminar patterns in Couette flow", *Physical review letters*, 94(1), 014502.

Brethouwer, G., Duguet, Y., & Schlatter, P., 2012, "Turbulent–laminar coexistence in wall flows with Coriolis, buoyancy or Lorentz forces", *Journal of Fluid Mechanics*, 704, 137-172.

Coles, D., 1965, "Transition in circular Couette flow", *Journal of Fluid Mechanics*, 21 (03), pp. 385-425.

Coles, D., 1966, "Progress report on a digital experiment in spiral turbulence", *AIAA Journal*, 4 (11), pp. 1969-1971.

Cros, A., and Le Gal, P., 2002, "Spatiotemporal intermittency in the torsional Couette flow between a rotating and a stationary disk", *Physics of Fluids*, 14(11), 3755-3765.

Duguet, Y., Schlatter, P., and Henningson, D. S., 2010, "Formation of turbulent patterns near the onset of transition in plane Couette flow", *Journal of Fluid Mechanics*, 650, 119-129.

Duguet, Y., and Schlatter, P., 2013, "Oblique laminar-turbulent interfaces in plane shear flows", *Physical review letters*, 110(3), 034502.

Fukudome, K., and Iida, O., 2012, "Large-Scale Flow Structure in Turbulent Poiseuille Flows at Low-Reynolds Numbers", *Journal of Fluid Science and Technology*, 7(1), 181-195.

Iida, O., and Nagano, Y., 1998. "The relaminarization mechanisms of turbulent channel flow at low Reynolds numbers. Flow", *Turbulence and Combustion*, 60(2), 193-213.

Ishihara, T., Hunt, J. C., and Kaneda, Y., 2011, "Conditional analysis near strong shear layers in DNS of isotropic turbulence at high Reynolds number", *In Journal of Physics*: Conference Series, 318, 4, p. 042004). IOP Publishing.

Jiménez, J., and Moin, P., 1991, "The minimal flow unit in near-wall turbulence", *Journal of Fluid Mechanics*, 225, 213-240.

Kim, J., Moin, P., and Moser, R., 1987, "Turbulence statistics in fully developed channel flow at low Reynolds number", *Journal of fluid mechanics*, 177, 133-166.

Manneville, P., 2011, "On the decay of turbulence in plane Couette flow", *Fluid Dynamics Research*, 43(6), 065501.

Manneville, P., 2012, "On the growth of laminar–turbulent patterns in plane Couette flow", *Fluid Dynamics Research*, 44(3), 031412.

Philip, J., and Manneville, P., 2011. From temporal to spatiotemporal dynamics in transitional plane Couette flow. *Physical Review E*, 83(3), 036308.

Prigent, A., Grégoire, G., Chaté, H., Dauchot, O., and van Saarloos, W., 2002, "Large-scale finite-wavelength modulation within turbulent shear flows", *Physical review letters*, 89(1), 014501.

Seki, D., Numano, T., and Matsubara, M., 2010, "Numerical and Experimental Investigations of Relaminarizing Plane Channel Flow", *In Seventh IUTAM Symposium on Laminar-Turbulent Transition,* pp. 367-372.

Seki, D., and Matsubara, M., 2012, "Experimental investigation of relaminarizing and transitional channel flows". *Physics of Fluids*, 24(12), 124102.

Shi, L., Avila, M., and Hof, B., 2013, "Scale invariance at the onset of turbulence in Couette flow", *Physical review letters*, 110(20), 204502.

Tsukahara, T., Seki, Y., Kawamura, H., and Tochio, D., 2005, "DNS of turbulent channel flow at very low Reynolds numbers", In: Proceedings of the Fourth International Symposium on Turbulence and Shear Flow Phenomena, Williamsburg, VA, USA, pp. 935-940.

Tsukahara, T., Iwamoto, K., Kawamura, H., and Takeda, T., 2006, "DNS of Heat Transfer in a Transitional Channel Flow Accompanied by a Turbulent Puff-like Structure", *In: Proceedings of the Fifth International Symposium on Turbulence, Heat and Mass Transfer*, pp. 193-196.

Tsukahara, T., and Kawamura, H., 2007, "Turbulent heat transfer in a channel flow at transitional Reynolds numbers", *In: Proceedings of the First Asian Symposium on Computational Heat Transfer and Fluid Flow*, Xi'an, China, p. 62.

Tsukahara, T., Kawaguchi, Y., Kawamura, H., Tillmark, N., and Alfredsson, P.H., 2010a, "Turbulence stripe in transitional channel flow with/without system rotation," *In: Seventh IUTAM Symposium on Laminar-Turbulent Transition,* Stockholm, Sweden, IUTAM Bookseries, Vol. 18, Springer, pp. 421-426.

Tsukahara, T., Tillmark, N., and Alfredsson, P. H., 2010b, "Flow regimes in a plane Couette flow with system rotation", *Journal of Fluid Mechanics*, 648, 5-33.

Tuckerman, L. S., Kreilos, T., Schrobsdorff, H., Schneider, T. M., and Gibson, J. F., 2014, "Turbulent-laminar patterns in plane Poiseuille flow", *Physics of Fluids*, 26(11), 114103.